Additivity of Capacitive and Inductive Coupling in Submicronic Interconnects

Jean-Etienne Lorival, Denis Deschacht, Yves Quéré, Thierry Le Gouguec, Fabrice Huret

HAL Id: lirmm-00093341
https://hal-lirmm.ccsd.cnrs.fr/lirmm-00093341

Submitted on 13 Sep 2006

Additivity of Capacitive and Inductive Coupling in Submicronic Interconnects

J.E. Lorival, D. Deschacht

Laboratoire d'Informatique de Robotique et de
Microélectronique de Montpellier
U.M.R. C.N.R.S. 5506,
161 rue ADA, 34392 Montpellier Cedex 5, France.
Deschacht@lirmm.fr

Y. Quere, T. Le Gouguec, F. Huret

Laboratoire d'Electronique et Systèmes de
Télécommunications
Université Bretagne Occidentale, UMR CNRS 2269,
6 Avenue le Gorgeu, BP809, 29285 Brest Cedex, France.

Abstract—**Constant evolution in integrated circuit technology has led to an increase in the switching speed of the digital chip. As a result, there is a growing interest in the inductance associated with signal lines. Inductive coupling effects on interconnects is an emerging concern in high performance digital integrated circuits. Based on an RLC transmission line model, associated to each propagation mode, a new crosstalk noise model is proposed to evaluate both the capacitive and the inductive coupling. The additivity of the coupling is shown and validated with several simulations.**

Keywords—coupling effects, inductive effects, on-chip interconnections, transmission lines, propagation modes.

I. INTRODUCTION

The signal integrity of many very large scale integration (VLSI) circuits is mainly degraded by the interconnect lines. Crosstalk noise has evolved as the key source of performance degradation and signal integrity problems in high speed VLSI designs. Various techniques have been proposed to evaluate the crosstalk noise in integrated circuits. Many waveform-approximation techniques or model-order reduction algorithms have been developed for the signal integrity verification of coupled interconnect lines. Reference [1] incorporates a model order reduction technique to efficiently simulate the on-chip interconnects as distributed RC sections. Until recently, most works have been limited to RC networks leaving an inherent unpredictability in the design process where inductive effects are suspected [2]. Operating frequencies that have increased over the past decade are expected to maintain this increasing behavior over the next decade approaching 10GHz by the year 2012. On-chip inductance is becoming increasingly important since integrated circuits now operate at frequencies where the inductive impedance of thick wide wires is comparable to the wire resistance. The importance of inductance in high performance VLSI design methodologies will increase as technologies downscale. In this paper, we highlight the importance of on-chip inductance modeling for crosstalk voltage evaluation by considering two parallel coupled interconnects. Based on

even and odd propagation modes, we evaluate the capacitive and inductive coupling part of the crosstalk noise.

The paper is organized as follows. The second section presents our approach to modeling RLC coupling noise waveforms. Based on an RLC transmission line model, associated to each propagation mode, we develop the respective capacitive and inductive part of the coupling and in section 3 we show the additivity of the coupling and validate it with SPICE simulations.

II. COUPLING MODELING

The first electrical cause of the crosstalk comes from a capacitive link between two lines, but the inductive effect increases with new technologies. Unfortunately, even for a simple two-line configuration, with only one cell, with self and mutual inductances and coupling capacitance, equations to model the noise pulse reach as high as the fifth order in the Laplace domain. These equations become computationally very difficult to calculate. So, it is difficult to determine an analytical expression for the crosstalk voltage.

The aim of this part is to find a predictive and simple analytical model of the crosstalk voltage in the case of two identical interconnects (Fig 1). We also check the additivity of capacitive and inductive coupling voltages.
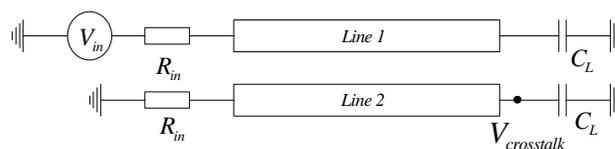
Fig. 1: Coupled-line model.

In the case of two parallel coupled transmission lines, two propagation modes exist: the even mode (e) or common mode and the odd mode (o) or differential mode. The configurations of these two propagation modes are illustrated on the following figure.

V_{in} is a voltage source, R_{in} represents the buffer equivalent resistances, in the real case, of the aggressor and the victim line; C_L the equivalent load capacitance.
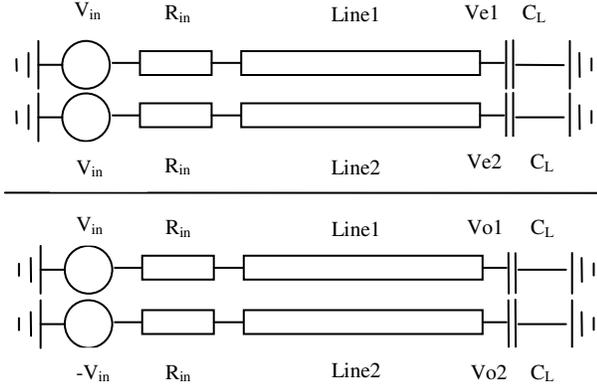
Fig.2: Coupled-line configurations for even and odd modes.

Then, the crosstalk voltage can be expressed as [3]:

$$V_{crosstalk} = \frac{V_e - V_o}{2} \tag{1}$$

where V_e and V_o are respectively the even and odd voltages. These voltages can be computed from the equivalent line models presented Fig 3. The principles of the analysis we have followed, in order to obtain the numerical values of the R, L, C, G equivalent parameters from which a set of coupled transmission lines can be modeled, have been presented in [4]. For the electrical simulations, we use the electrical parameters determined by parametric extraction with Full-Wave Electromagnetic Analysis for a frequency of 1 GHz. R, L, C, G can be expressed by a matrix where the element ii represents the eigen effect and the indicator ij the coupled effects. In the structures we study, both the conductance G and R_{12} are negligible. The per unit length (p.u.l) parameters RLC of equivalent line (Fig 4) for each mode are computed from the p.u.l. parameters of the coupled lines (2).
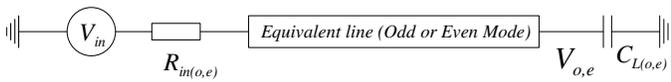
Fig. 3 : Equivalent line model for even (common) or odd (differential) propagation modes.
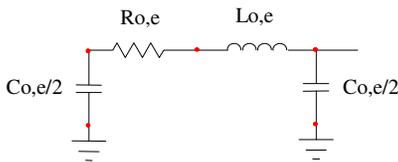
Fig 4 : p.u.l. RLC model for even or odd modes.

$$\begin{pmatrix} R_e \\ R_o \end{pmatrix} = \begin{pmatrix} R_{11}/2 \\ 2R_{11} \end{pmatrix} \quad \begin{pmatrix} L_e \\ L_o \end{pmatrix} = \begin{pmatrix} (L_{11}+L_{12})/2 \\ 2(L_{11}-L_{12}) \end{pmatrix} \quad \begin{pmatrix} C_e \\ C_o \end{pmatrix} = \begin{pmatrix} 2C_{11} \\ (C_{11}+2C_{12})/2 \end{pmatrix} \tag{2}$$

We can thus transpose the crosstalk voltages of each model, *ie* RLC, C and L, into modal voltage. The modal characteristic impedances (Z) and propagation factors (γ) of RLC model are presented below.

$$Z_{RLCe} = \sqrt{\frac{R_{11} + j(L_{11} + L_{12})\omega}{jC_{11}\omega}} \tag{3a}$$

$$\gamma_{RLCe} = \sqrt{(R_{11} + j(L_{11} + L_{12})\omega)\,jC_{11}\omega} \tag{3b}$$

$$Z_{RLCo} = \sqrt{\frac{R_{11} + j(L_{11} - L_{12})\omega}{j(C_{11} + 2C_{12})\omega}} \tag{4a}$$

$$\gamma_{RLCo} = \sqrt{(R_{11} + j(L_{11} - L_{12})\omega)\,j(C_{11} + 2C_{12})\omega} \tag{4b}$$

In opposition of [3], in this work, the coupling capacitive part (C-model) is obtained by using a simple RC distributed model ($L_{11} = L_{12} = 0$) and the inductive part (L-model) with only $C_{12} = 0$. We obtain then:

$$Z_{C_e} = \sqrt{\frac{R_{11}}{jC_{11}\omega}} \;;\; Z_{C_o} = \sqrt{\frac{R_{11}}{j(C_{11} + 2C_{12})\omega}} \tag{5a}$$

$$\gamma_{C_e} = \sqrt{jR_{11}C_{11}\omega}\,; \gamma_{C_o} = \sqrt{jR_{11}(C_{11} + 2C_{12})\omega} \tag{5b}$$

$$Z_{L_e} = \sqrt{\frac{R_{11}+j(L_{11}+L_{12})\omega}{jC_{11}\omega}}\,; Z_{L_o} = \sqrt{\frac{R_{11}+j(L_{11}-L_{12})\omega}{jC_{11}\omega}} \tag{5c}$$

$$\gamma_{Le} = \sqrt{(R_{11} + j(L_{11} + L_{12})\omega)jC_{11}\omega} \tag{5d}$$

$$\gamma_{Lo} = \sqrt{(R_{11} + j(L_{11} - L_{12})\omega)jC_{11}\omega} \tag{5e}$$

One should note that characteristic impedances and propagation factors of even RLC and L models are equal, leading to:

$$V_{RLCe} = V_{Le} \tag{6}$$

For on-chip interconnects, in the odd mode, the relation $R_{11} \gg (L_{11} - L_{12})\omega$ is generally verified, so, according to propagation factors and characteristic impedances of each mode and model, we can write (6).

$$V_{RLCo} = V_{Co} \; ; \; V_{Ce} = V_{Lo} \qquad (7)$$

The relations (1), (5,) (6) and (7) lead to a simple crosstalk voltage expression and the check of the additivity of capacitive and inductive coupling voltages (8a-8d).

$$V_{crosstalk(RLC)} = \frac{V_{RLC_e} - V_{RLC_o}}{2} \qquad (8a)$$

$$= \frac{V_{L_e} - V_{C_o}}{2} \qquad (8b)$$

$$= \frac{V_{C_e} - V_{C_o} + V_{L_e} - V_{Lo}}{2} \qquad (8c)$$

$$V_{crosstalk(RLC)} = V_{crosstalk(C)} + V_{crosstalk(L)} \qquad (8d)$$

III. COMPARISON WITH SPICE SIMULATIONS

We have shown that the crosstalk resulting from the total coupling (capacitive + inductive) could be written as the sum of the coupling where V_C and V_L are the capacitive coupling and the inductive coupling parts respectively on the crosstalk voltage. We will now compare the far-end crosstalk voltage obtained from coupled-line configuration (Fig. 1) with the results given by equation (8d).

The interconnect lines are described by their electrical parameters. For typical submicron geometry, the electrical parameters obtained by electromagnetic analysis [4], are used to build the distributed π-RLC model in the electrical simulations, (Fig. 5).
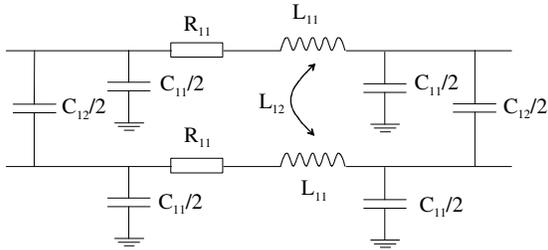
Fig. 5: Elementary cell for coupled-line π-model.

As an example, the per unit length value applied on the model passive components are 71.84Ω/mm for the line resistance R_{11}, 46.3fF/mm and 35.1fF/mm for the line capacitor C_{11} and the interline capacitor C_{12}, 1.4614 nH / mm, L_{11} = 1.4614 nH / mm and L_{12} = 1.1231 nH / mm for the self and mutual inductance respectively. The voltage source V_{in} is a 1V step function, R_{in} and C_L are equal respectively to 50Ω and 10fF. All the simulations are realized with a 5mm length line.

The configuration where the aggressor line is attacked by a voltage step corresponds to the case where the inductive effect is the most important. To verify the simplifications detailed by (7) when the line resistance is most important than the line reactance, the capacitive and the inductive output voltages obtained depending on how the different propagation modes are compared each other. Fig. 6 shows the comparison between the victim line output waveform of the coupled-line configuration exposed Fig.2 and the capacitive coupling waveform for the odd mode.
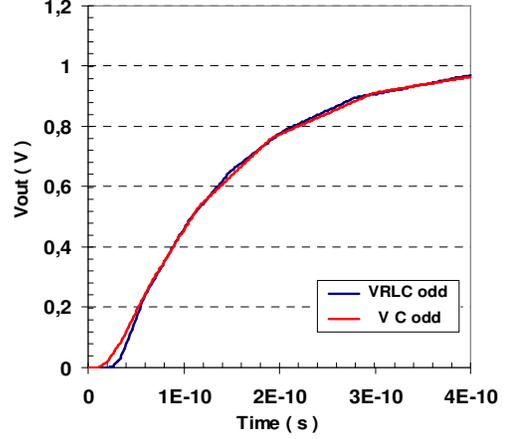
Fig. 6: V_{RLCO} and V_{CO} waveforms comparison.

The two waveforms are equivalent. This connection must be now verified between the inductive voltage taken in the odd mode and the capacitive voltage considered in the even mode; the result is exposed via the following figure.
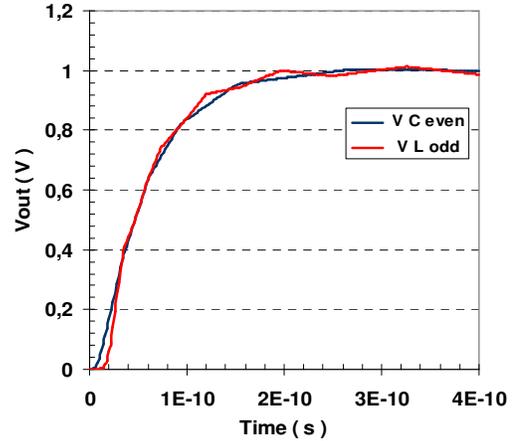
Fig. 7: V_{CE} and V_{LO} waveforms comparison.

The two comparisons show good agreement between the waveforms. The relation (7) being verified, both the capacitive and the inductive crosstalk voltage can be deduced from (1) that says:

$$V_{crosstalk}(C) = \frac{Vc_{even} - Vc_{odd}}{2} \qquad (10a)$$

$$V_{crosstalk}(L) = \frac{V_{L\,even} - V_{L\,odd}}{2} \qquad (10b)$$

The sum of these two crosstalk waveforms is then compared with the crosstalk voltage obtained by simulating the coupled-line model configuration Fig.1. The agreement between the two crosstalk voltages as well as the inductive and the capacitive crosstalk voltage are illustrated Fig.8.
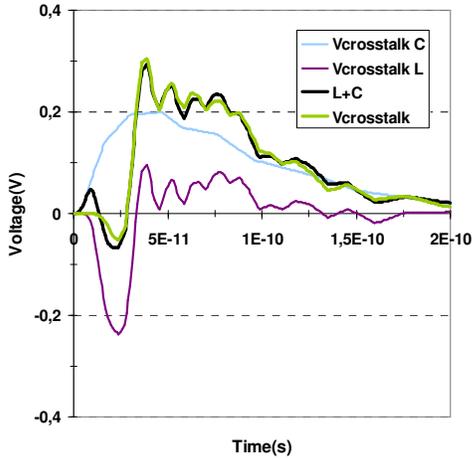
Fig. 8: Comparison between the simulated crosstalk voltage and the one obtained by the coupling effects sum.

For a LH transition, at the line beginning, the capacitive coupling noise has a positive polarity whereas the inductive coupling noise has a negative one. The sum of the coupling effects gives as a result a positive crosstalk waveform. By analysing the previous figure, a good agreement between the two crosstalk voltages (named $V_{crosstalk}$ and L+C) can be observed. As a consequence, the coupling effects are additive and the expression (8d) can be applied to determine the crosstalk voltage.

This equivalence in crosstalk voltage evaluation have been verified when, by considering still the previous parametric values, the line resistance value has been divided by 2.
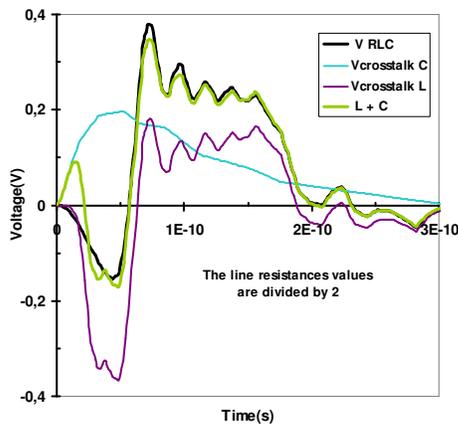
Fig. 9: Comparison between the RLC crosstalk voltage and the one obtained by the coupling additivity, R_{11} of simulation Fig. 8 divided by 2.

Other validations can be realized by keeping the parametric values used for the experimental crosstalk evaluation Fig. 8 like increasing by 2 the self and the mutual inductances values (Fig. 10) and divided in the same time the line resistance value (Fig. 11), leading in to a dominant inductive coupling and to a loseless LC coupled-line structure.
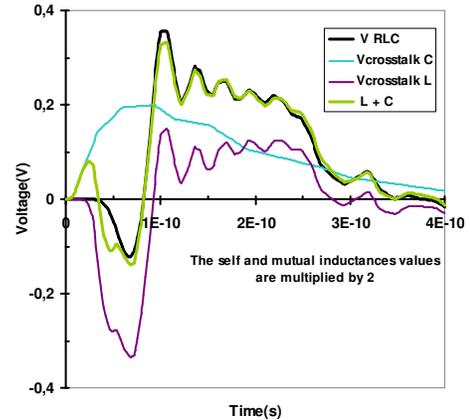
Fig. 10: Comparison between the RLC crosstalk voltage and the one obtained by the coupling additivity, L_{11} and L_{12} values from simulation Fig. 8 doubled.
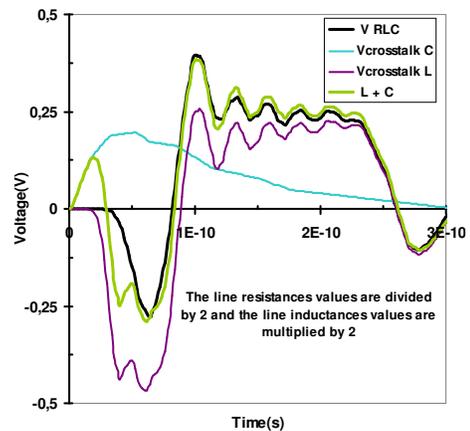
Fig. 11: Comparison between the RLC crosstalk voltage and the one obtained with the coupling additivity by reducing by half R_{11} and doubled L_{11} and L_{12} values.

Whatever the structure geometry considered, whatever the coupling being dominant compared to the other, the agreement between the total crosstalk voltage (simulated with the RLC distributed coupled-line structure) and the one resulting from the coupling additivity (simulated with the single line distributed equivalent model by investigating the propagation modes) is very good.

Other comparisons have been realized by taking into account different resistances, capacitances and inductances values for different coupling lengths, the aggressor line

being attacked by a 1V step with different transition times tr. The additivity of the coupling effect could have been verified in all the cases. The next figure presents the comparison between the simulated crosstalk with the reference configuration and the crosstalk resulting from both the capacitive and inductive crosstalk voltage additivity for a 3mm length line when the aggressor line is attacked by a 1V step voltage with a 25ps transition time. The line resistance is equal to $R_{11}=47.9\Omega/mm$, the line capacitance and the interline capacitance are defined as $C_{11}=52.4fF/mm$ and $C_{12}=30.9fF/mm$. At last, the self and mutual inductances are respectively equal to $L_{11}=1.6nH/mm$ and $L_{12}=1.2nH/mm$. The buffer equivalent resistance and the load capacitance have the same value than previously.

The resistance value has been decreased, corresponding to a line for which the width is higher, whereas the self and mutual inductances have been both increased to tend to an unfavourable case of the relation $R_{11} >> (L_{11}-L_{12})\omega$.
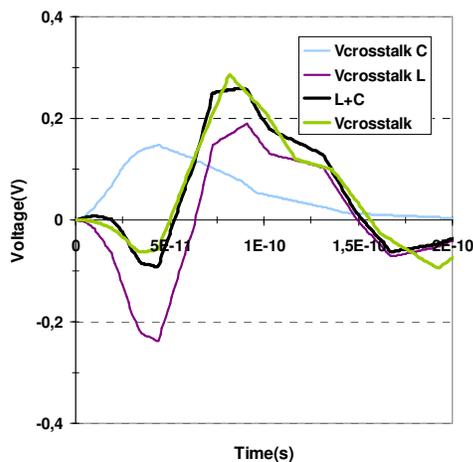
Fig. 12: Comparison between the simulated crosstalk voltage and the one obtained by the coupling effects sum with the new parameters and configuration description.

The agreement between the simulated crosstalk and the one depending on the coupling effects additivity is very good; the additivity being still verified.

IV. CONCLUSION

For new technology generation, the reactance is comparable to the resistance value and tends to become the dominant component as we scale down towards 50nm. Therefore, it is imperative that high performance wire analysis includes RLC networks to describe signal wires. In this paper, a new crosstalk voltage expression is presented based on both the common (even) and differential (odd) propagation modes. The capacitive and the inductive parts of the crosstalk voltage have been evaluated, and we have shown that the resulting crosstalk, corresponding to the total one, could be written as the sum of the coupling effects

when, in the odd mod, it can be verified that the reactance is smaller than the resistance.

REFERENCE

[1] K. Shepard et al, "Globalharmony: Coupled noise analysis for full-chip RC interconnect networks", in Proc. IEEE/ACM Int. Conf. Computer-Aided Design, Nov1997, pp. 139-146.

[2] P. Heydari, M. Pedram, « Capacitive Coupling Noise in High-Speed VLSI Circuits » IEEE Trans. On CAD of I.C. and S., Vol 24, n 3, March 2005, pp.478-488.

[3] K. Agarwal, D. Sylvester, D. Blaauw, "A Simplified Transmission-Line Based Crosstalk Noise Model for On-Chip RLC Wiring", in Proc. ASP-DAC, 2004, pp. 858-864.

[4] F. Huret, D. Deschacht, G. Servel, P. Paleczny, J.F. Legier, P. Kennis, "Full Wave analysis of conductor and substrate losses in high speed VLSI interconnects", in Proc. 30th European microwave conference 2000, Paris, October, 3-5, 2000.

[5] J.F. Lee, D.K. Sun, Z.J. Cendes, "Full wave analysis of dielectric waveguides using tangential vector finite elements." IEEE Trans. Microwave Theory Tech., Vol. MTT-39, N°8, August 1991.